Impact of Curing Temperature on Microstructures and Properties of Isobutylene–Isoprene Rubber/Clay Nanocomposites

Yong-Lai Lu,[1] Zhao Li,[2] Li-Xin Mao,[2] Yao Li,[2] You-Ping Wu,[1] Yu-Rong Liang,[2] Li-Qun Zhang[1,2]

[1]*Key Laboratory for Nanomaterials, Ministry of Education, Beijing University of Chemical Technology, Beijing 100029, People's Republic of China*
[2]*Key Laboratory of Beijing City on Preparation and Processing of Novel Polymer Materials, Beijing University of Chemical Technology, Beijing 100029, People's Republic of China*

Received 6 October 2007; accepted 11 May 2008
DOI 10.1002/app.28690
Published online 10 July 2008 in Wiley InterScience (www.interscience.wiley.com).

ABSTRACT: In this work, the influence of curing temperature on microstructures of isobutylene–isoprene rubber/clay nanocomposites (IIRCNs) prepared by melt compounding was characterized using wide-angle X-ray diffraction and TEM. The gas barrier and tensile properties of IIRCN cured under different temperature were examined. The results reveal that high pressure, curing reactions, and reactions of amine intercalants with curing agents together play important roles on determining the final microstructures of cured IIRCNs. Changing curing temperature would dramatically alter intercalated structure, dispersion homogeneity, filler–rubber interaction strength, and crosslinking density of obtained IIRCN, resulting in great difference in final properties. Finally, some suggestions for the preparation of successful RCNs were proposed. © 2008 Wiley Periodicals, Inc. J Appl Polym Sci 110: 1034–1042, 2008

Key words: clay; nanocomposites; rubber; vulcanization

INTRODUCTION

Very recently, increasing attention has been paid on rubber/clay nanocomposites (RCNs). Present works[1] have demonstrated that the reinforcing effect of nanodispersed clay layers on rubber matrix is comparable to that of the conventional reinforcing filler (i.e., carbon black). The strength of non–strain-induced crystallization of rubber reinforced by nanoclay layers can exceed 20 MPa, which is 10–15 times higher than that of pure matrix rubber. RCNs also exhibit some other significantly improved performances in gas barrier, swelling resistance, and heat resistance.[1–3]

The most important consideration to achieving successful RCNs is the dispersion of clay particles in the rubber matrix. With the use of clay as filler, generally, three types of composites materials may be obtained: conventional composites, intercalated nanocomposites, and exfoliated nanocomposites. Among all three types, the exfoliated clay is the optimum situation in terms of polymer reinforcement.[1,4,5] However, fully exfoliated RCNs are not at all easy to produce.[1] To the authors' knowledge, in most of the reported RCNs prepared by melt compounding, full exfoliation of clay layers in the rubber matrix could not be achieved. Some previous work has revealed that the dispersion state of clay in a rubber matrix is influenced by the type of intercalants,[6–10] compounding condition (shear rate and temperature),[9–11] and polarity of the matrix rubber,[12–14] which is similar to the case of intensively studied thermoplastic polymer/clay nanocomposites (TP-PCNs).[4,5] Different from TP-PCNs, RCNs need a vulcanization process (i.e., curing) following nanocompounding of rubbers and clay to obtain the crosslinked composites. It was found that the microstructures of some RCNs were dramatically changed by the vulcanization. Our previous works[15–17] on isobutylene–isoprene RCNs (IIRCNs) discovered that the pressure and heat during vulcanization should play important roles on microstructural changes of RCNs; and high pressure results in intensive aggregation of initially fine-dispersed clay particles and the formation of large clay agglomerates in cured RCNs. Other researchers have also studied this problem but focused on the effects of curing reactions.[13,18–22]

To minimize the negative effect of high pressure on the microstructure, we performed the vulcanizations

Correspondence to: L.-Q. Zhang (zhanglq@mail.buct.edu.cn).
Contract grant sponsor: National Tenth-Five Program; contract grant number: 2001BA310A12.
Contract grant sponsor: Beijing Nova Program; contract grant number: 2006A15.
Contract grant sponsor: National Nature Science Foundations of China; contract grant numbers: 50173003, 50303002.
Contract grant sponsor: National Outstanding Youth Science Fund; contract grant number: 50725310.

TABLE I
Formulation for IIRCN compound in this Work

Materials	Loading (phr[a])
IIR	100
Zinc oxide (ZnO)	5
Steric acid (SA)	2
Tetramethyl thiuram disulfide (accelerator TMTD)	1.0
2-Mercapto benzothiazole (accelerator M)	0.5
Sulfur (S)	1.8
N-phenyl-α-naphthylamine (antioxidant A)	1.0
OMC	10

[a] phr is the abbreviation of weight parts per 100 weight parts of rubber.

of IIRCNs under atmospheric or low pressure (i.e., ~ 3 MPa); which resulted in nanocomposites with improved dispersion state and considerably good gas barrier and mechanical properties compared to the control samples cured under high pressure (i.e., ~ 15 MPa).[15,23] However, high-pressure vulcanization is necessary for some rubber products having complicated shape, so that the above method cannot be commonly applied. It was expected that the spatial aggregation of clay particles in rubber matrix caused by high pressure should mainly happen within the initial period of curing course, when most of rubber chains are in flowing state. Therefore, increasing curing rate at elevating temperature might be a feasible means to reduce the negative effect of high pressure. In this work, the influence of curing temperature on microstructures and properties of IIRCNs prepared by melt blending was investigated. Some novel and interesting phenomena were observed. Finally, some suggestions for preparing successful RCNs based on organically modified clay (OMC) were proposed according to our findings in this work.

EXPERIMENTAL

Material and formulation

IIR (Polysar301) was provided by North Special Rubber of Hengshui (Hebei Provinice, China). The OMC (Nanomer® I.30E) with an initial basal spacing of ~ 2.2 nm was obtained by Nanor, USA. Other materials and reagents used in this work are commercial products. The formulation for IIRCN compound (i.e., uncured composites) is described in Table I.

Preparation of nanocomposites and samples

IIR and OMC were first compounded for ~ 15 min using an Φ 152.4 mm two-roll open mill. The additives, ZnO, SA, S, accelerators, and antioxidant were then generally mixed. Some compounds without any curing agents (CAs) were reserved for experiment of high-pressure thermal treatment. The calendered IIRCN compound sheet of 1 mm in thickness and 200 mm in width was removed from rotating roll. Some of them were used for wide-angle X-ray diffraction (WAXD) and TEM examinations. The other compounds were cured on a hot press at different temperatures ranging from 110 to 180°C with an interval of 10°C under 15 MPa pressure for their optimum cure times (i.e., T_{90}) determined by using a disc oscillating rheometer (P335B2, Beijing Huanfeng Chemical Technology and Experimental Machine Plant, China). In brief, the IIRCNs cured at different temperatures were denoted by IIRCN110, IIRCN120, IIRCN130, IIRCN140, IIRCN150, IIRCN160, IIRCN170, and IIRCN180, respectively. The IIRCN compound without CAs was thermally treated at 15 MPa and 110 or 180°C for 1 h on a hot press.

The mixture of OMC and CA system was prepared by solution mixing. The CA system includes activation agents (ZnO and SA), crosslinking agents (accelerator TMTD and accelerator M), and crosslinking agents (sulfur). The usage formation of OMC and CA is same as that for the IIRCN described in the table. The mixture of OMC and CA was dried in a vacuum oven under 50°C for 72 h ensuring that the residual solvent was removed completely. After drying, the mixture was stored in a vacuum oven under 110, 160, and 180°C, respectively, for 1 h, and then cooled to room temperature in vacuum environment.

Characterization and measurements

The smooth specimens for WAXD experiments with a dimension of 18 × 20 × 1 mm^3 were cut from uncured and cured IIRCN sheets. WAXD measurements were carried out on a Rigaku RINT diffractometer with a Cu Kα radiation (40 kV, 200 mA) at the scan rate of 1°/min. Ultrathin sections of uncured and cured IIRCNs were cut using a microtome at about ~ 100°C for TEM experiments and collected on the copper grid. TEM observations were performed on an H-800-1 transmission electron microscope (Hitachi, Japan) with an acceleration voltage of 200 kV. The nitrogen permeability of cured IIRCN at 23°C was determined by previously reported method.[24] The tensile properties of cured IIRCNs at 25°C ± 2°C were examined according to the ISO standard (ISO 7619).

RESULTS AND DISCUSSION

Curing behaviors of IIRCNs at different temperatures

Figure 1 represents great influence of temperature on curing behaviors of IIRCNs. It was usually believed that the intercalated structure and spatial

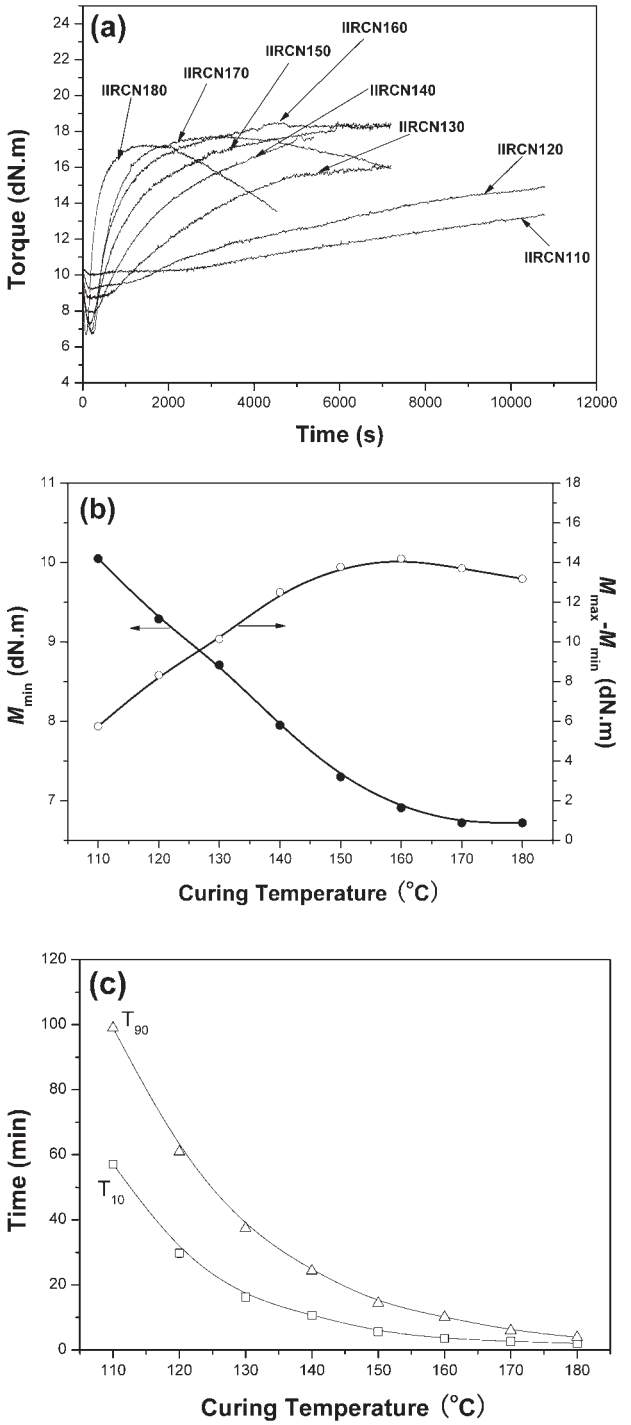

Figure 1 Vulcanization behaviors of IIRCN (IIR : OMC = 100 : 10) under different temperatures: (a) vulcanization curves; (b) minimum torque (M_{min}), and maximum torque (M_{max}); (c) T_{10} and T_{90}.

distribution of nanoclay particles could be changed at large extant during initial period of curing course, when the crosslinking density is relatively low, and the compound has high flowing ability. Minimum torque (M_{min}) is qualitatively in reverse proportion to the flowing ability of rubber compounds during initial curing period. As shown in Figure 1(b), the value of M_{min} decreases from $\sim$ 10 to 6.7 dN m with curing temperature increasing from 110 to 180°C. Lower viscosity or higher flowing ability of the compound would facilitate the microstructural changes of the composite.[16]

On the other hand, the changing extent in microstructures of the RCN during curing course is also strongly determined by the length of the period when the rubber compound has low viscosity. It was imaged that the microstructures of the RCN would be fixed when crosslinking density of the matrix rubber reaches some certain level. As well to known, the crosslinking density of rubber vulcanizates is not high, and in the range of $\sim 10^{-4}$ to 10^{-5} mol/cm^{-3}, so that the rubber chains still maintain relatively high motion ability even though the curing degree is quite high. As a result, it cannot be affirmed exact time when microstructures of RCN could be fixed during curing course at present. We are carrying out the study on this problem and will report the result in the future article. In rubber industry, T_{10} and T_{90} are two important curing parameters extracted from the curing curve. T_{10} (i.e., scorch time) is the time when the torque reaches 10% of the difference between the difference between the maximum and the minimum torques ($M_{max} - M_{min}$). Below T_{10}, the crosslinking density is so low that the rubber compounds can flow and be molded. It was expected that the microstructure of RCNs would change at large extent during scorch safety period (i.e., below T_{10}) due to very low crossliking density of matrix rubber. It can be seen from Figure 1(c) that the value of T_{10} dramatically reduces with curing temperature; and T_{10}s for 110–140°C curing courses are far longer than those for 150–180°C ones. For instance, the T_{10} for 110°C curing is about 28 times as long as that for 180°C curing. T_{90} (i.e., optimal curing time) is the time when the torque reaches 90% of $M_{max} - M_{min}$. The crosslink density at T_{90} is usually the best degree for most rubber composites. The difference between T_{90} and T_{10} ($T_{90} - T_{10}$) is inversely proportional to the curing speed. Figure 1(c) displays that the $T_{90} - T_{10}$ dramatically decreases with curing temperature increasing,. For example, the $T_{90} - T_{10}$ for 110°C curing is about 22 times as large as that for 180°C. The faster the curing speed, the shorter the period allowing the microstructure of the RCN changing, especially for spatial distribution of the clay particles.

From the above analysis, we could draw a conclusion that altering curing temperature would result in much larger change in curing course such as scorch time (T_{10}) and curing speed than that in viscosity of the compound. If only curing behaviors under different temperatures are considered, increasing curing temperature should depress the microstructural changes of RCNs during curing process.

The difference between maximum torque (M_{max}) and M_{min} ($M_{max} - M_{min}$) can be used to represent the crosslinking density of the rubber composite qualitatively. Figure 1(b) shows that the value of $M_{max} - M_{min}$ increases first with temperature elevating and then slightly drops down after reaching maximum value at 160°C. Curing curves for IIRCN170 and IIRCN180 in Figure 1(a) suggest that the decrease in $M_{max} - M_{min}$ at 170 and 180°C should be due to the vulcanization reversion. Therefore, the crosslinking density of the IIRCN increases with curing temperature at the range of 110–160°C and then slightly decreases.

Influence of curing temperature on microstructures of IIRCNs

Figure 2 displays WAXD patterns and corresponding TEM images of uncured RCN and RCNs cured at different temperatures with ~ 15 MPa pressure. The results reveal that both intercalated structures and spatial dispersion of OMC particles were greatly affected by curing temperature. In the WAXD pattern of uncured IIRCN, there is a sharp reflection peak corresponding to a basal spacing of 3.24 nm and its high order reflections (1.61 and 1.05 nm) are obvious, representing the existence of intercalated structures with high-order degree. In the WAXD pattern of IIRCN110, there is a more sharp reflection corresponding to a basal spacing of 5.20 nm, which reveals that vulcanization at 110°C results in further intercalation of IIR chains into clay galleries and intercalated clay layers stacking more orderly. There are also three reflections at high 2θ angle, which should be mainly attributed to higher order reflections for basal one at 5.20 nm, although their locations, especially for two reflections at 2.80 and 1.82 nm, somewhat depart from the "right" positions (calculated) of high-order reflections. In the WAXD patterns of IIRCN140, IIRCN160, and IIRCN180, there are two reflections: (1) the reflection peak corresponding to the basal spacing around 5.0 nm indicating further intercalation during curing; (2) the reflection peak corresponding to the other basal spacing of ~ 1.30 nm, which is close to the value of pristine sodium montmorillonite.[14,25] The reflections at ~ 5.0 nm is considerably broad compared with IIRCN110. Moreover, the intensity of peaks at ~ 5.0 nm becomes weaker referring to that of at ~ 1.30 nm with curing temperature elevating. These results suggest that high curing temperature would facilitate deadsorption of the organic amine intercalants with the formation of pristine clays, and this deadsorption would be more remarkable when curing temperature is beyond 140°C. In TEM images [Fig. 2(b)], there are three types of dispersions: (1) granular and very dark dispersion representing ZnO particles; (2) large dark dispersion representing large clay agglomerates; (3) small gray dispersion representing rich area of fine dispersed nanoclay layers. In the IIRCN110, the amount of clay agglomerates increases and that of fine dispersed nanoclay layers decreases compared with uncured IIRCN. The dispersion state of clay in IIRCN140 or IIRCN160 is considerably better than that in uncured IIRCN or IIRCN110: the dimension of clay agglomerates decreases and fine-dispersed nanoclay layers are much more. Moreover, the dimension of dispersed clay particles in IIRCN160 is smaller compared to IIRCN140. These results suggest that the further intercalation (i.e., clay gallery height increasing) should take place during the initial period of curing course and could improve the dispersion state of clay particles. At low-curing temperature (i.e., 110°C), the scorch period is very long, that is, to say, the rubber compound would maintain following state during long period; and as a result, intercalated clay layers with increasing gallery height aggregate again with the formation of large clay agglomerate due to high-pressure effect.[15–17] If the crosslinking rate is accelerated by elevating curing temperature and the period for rubber compound having flowing ability is reduced, this aggregation would be retarded and the improved dispersion of clay particles could be maintained. The dispersion state of clay in IIRCN180 is improved compared with IIRCN110 and uncured IIRCN, but worse than that in IIRCN160. The intensive deadsorption of intercalants when curing temperature exceeding 160°C generates large amount of inorganic clay particles, which are far more incompatible with IIR matrix than OMC, and therefore, easy to aggregate. Of course, high crosslinking reaction rate resulted from high-curing temperature can retard not only the aggregation of inorganic clay particles, but also the further intercalation of IIR chains to the silicate gallery. It can be seen from Figure 2(a) that the gallery height increase of interacted clay in IIRCN180 (~ 1.62 nm) is obviously smaller than that in IIRCN110, IIRCN140, and IIRCN160 (1.96–1.79 nm).

To distinguish the effects of heat and pressure from that of curing reactions, the IIRCN compounds without any CAs were thermally treated at 110 or 180°C under 15 MPa for 1 h. The WAXD patterns of treated IIRCNs and pure OMC are shown in Figure 3. High-pressure thermal treatment at 110°C caused deintercalation of IIR chains with the formation of new intercalated structures with smaller gallery height. This result reveals that the further intercalation happening in initial curing period is solely related to curing reactions. In the WAXD pattern of the sample after high-pressure thermal treatment at 180°C, two reflections at 2.73 nm and 2.25 nm are obvious, but the reflection corresponding to pristine clay does not apparent. This

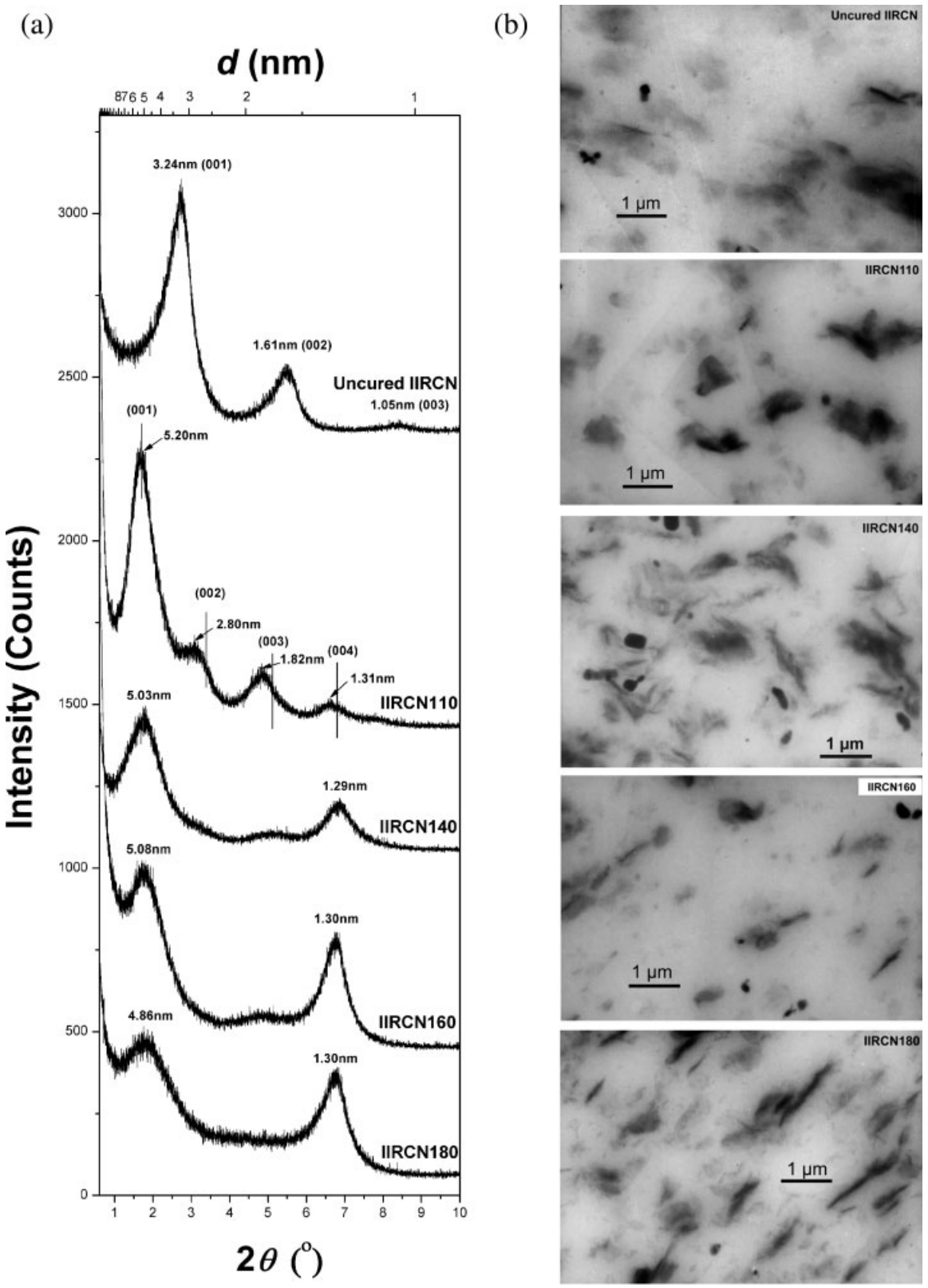

Figure 2 (a) WAXD patterns and (b) TEM images of IIRCNs (IIR : OMC = 100 : 10) cured at different temperatures. WAXD curves were shifted vertically for clarity.

result suggests that the severe deadsorption of intercalants during curing course at high temperature (i.e., 160–180°C) should have nothing to do with heat and pressure during curing process.

For further understanding the mechanism of deadsorption of intercalants, WAXD patterns of the mixture of OMC and CA treated under different temperatures were tested, as shown in Figure 4. In the pattern of untreated mixture of OMC and CA, there is a basal reflection at ~ 3.55 nm, which is obviously larger compared to pure OMC. This could be attributed to the intercalation of CA into the gallery of OMC with solution mixing. After 1-h thermal treatments under 110°C, the position of the basal spacing shifted to 6.89 nm, and the reflection peak became broader and weaker, which suggests that high-temperature treatment would lead to further intercalation and disturb ordered stacking of clay layers in the intercalated structure. It can also be found that basal reflection peak became more and more broad and week with the temperature of thermal treatment increasing from 110 to 180°C, although the peak position decreased from 6.89 nm to 3.53 nm. This result implied that high temperature of thermal treatment might facilitate further intercalation and resulted in delamination of more

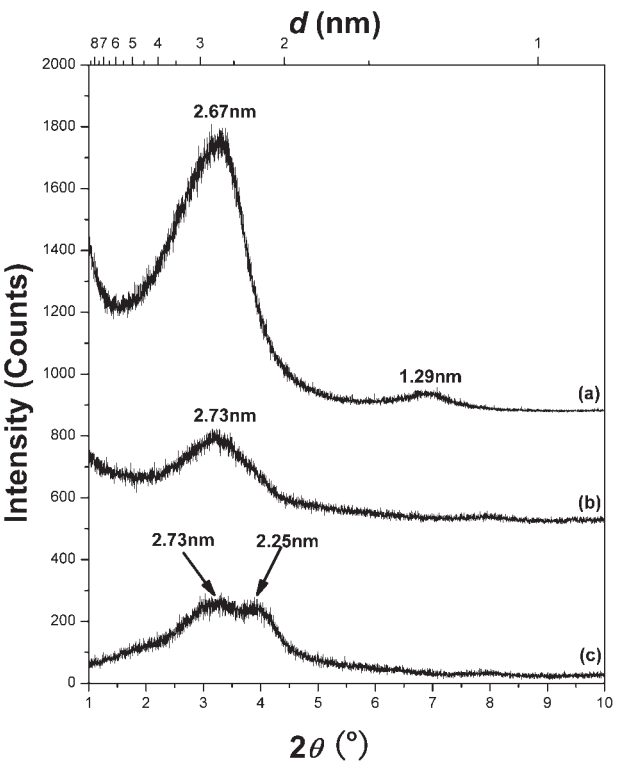

Figure 3 WAXD patterns of (a) OMC; (b) IIRCN without curing agents after 60-min thermal treatment at 110°C and 15 MPa; (c) IIRCN without curing agents after 60-min thermal treatment at 180°C and 15 MPa. WAXD curves were shifted vertically for clarity.

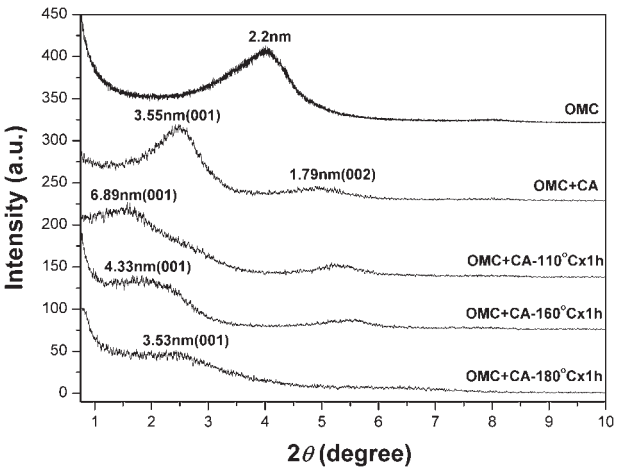

Figure 4 Influence of treating conditions on WAXD patterns of the mixture of OMC and curing agents (CA). The WAXD patterns of pure OMC and untreated mixture of OMC and CA were also plotted for a comparison.

amounts of clay layers. We assumed that intercalants could react with CAs during high-temperature treatments, which induced inserting of CA molecules into the gallery of OMC. It should be noticed that the reflection corresponding to pristine clay is not observed in the WAXD patterns of all treated mixture of OMC and CA, indicating that the reactions between intercalants and CA cannot directly lead to the deadsorption of intercalants. Some other researchers[13] previously suggested that this kind of reactions might yield deintercalation of the clay galleries or their delamination. We proposed a new mechanism of deadsorption of intercalants as following. During curing process of IIRCN, some parts of CA would first react with the intercalants, and some intermediate compounds would form within the gallery of intercalated clay structure, which only results in gallery height increase or delamination of clay layers. These intermediate compounds would also react with IIR out of the interlaced structure, causing that some intercalants would be extracted from OMC and some inorganic clay would be formed after curing process. Higher curing temperature could result in more amounts of the intercalants reacting with CA system, so that more amounts of them might be extracted out of the intercalated clay structures by reactions between the intermediate compounds with rubber. Of course, the reactions between the intermediate compounds with IIR chains within the gallery would result in gallery height increasing compared to uncured IIRCN compounds. Usuki and Kato[19] brought out an assumption that the modification of rubber chains caused by their reactions with polar-curing accelerator reagents in the initial curing period would lead to the further intercalation. In the case of IIRCN, this possibility might also exist.

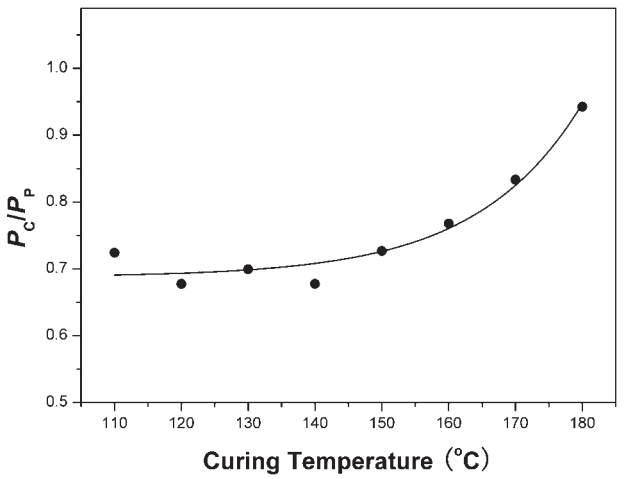

Figure 5 Impact of the curing temperature on the gas barrier property of cured IIRCN (IIR : OMC = 100 : 10). P_c and P_p represent the gas permeability of the composite and pure matrix rubber, respectively. The gas permeability for pristine IIR cured at 110 and 180°C are 3.64 and 3.67 × 10^{-18} m^2 s^{-1} Pa^{-1}, respectively, the average value of which was used as the gas permeability for pristine IIR.

Influence of curing temperature on properties of IIRCNs

Figure 5 plots the relative gas permeability of IIRCNs (P_c/P_p) as a function of curing temperature. In the range of 110–150°C, the gas-barrier property of IIRCN changed little with curing temperature. When the curing temperature is over 160°C, it decreased abruptly with curing temperature. The gas-barrier property of PCNs is determined by the dispersion state of clay layers and their interactions with polymer matrix.[26,27] Fine dispersion of clay layers would prolong the pathway for gas molecules traveling in the composite, and therefore, increase the gas-barrier property. The inorganic clay, having poor interaction with matrix polymer, results in the microcavities in the interface,[28] which would decrease the gas-barrier property.[26,27] Within the region of 110–150°C, increasing curing temperature improves the dispersion state and also increase the amount of inorganic clay due to the reactions of intercalants with CAs. As the result of trade-off of these two factors, the gas barrier properties of IIRCNs cured under this temperature region are slightly different. However, higher curing temperatures (i.e., 160–180°C) cause more intercalants reacting with CAs with producing large amount of inorganic clays, finally resulting in obvious decrease in gas-barrier property.

Table II represents the strong influence of curing temperature on the tensile properties of IIRCNs. As it is widely known that the modulus at small elongation of the rubber vulcanizate is dominantly proportional to its crosslinking density,[29] whereas that at high elongation is mainly related to filler–rubber interaction.[30,31] In this article, therefore, the reinforcement index (α) of the nanoclay particle defined as the ratio of modulus at 500% strain to that at 50% strain (M500/M50) was used to represent the strength of interfacial interaction between nanoclay layers and IIR. The impact of the curing temperature on the value of α of IIRCN is shown in Figure 6. It can be seen that it first increased with curing temperature and then dropped down when it is over 160°C. TEM investigation [Fig. 2(b)] has revealed that the dispersion state of clay particles was improved with curing temperature elevating in the range of 110–160°C, which increased the effective contact area between clay layers and IIR and therefore enhanced their interfacial interactions. On the other hand, WAXD study displays that high-curing temperature would cause formation of inorganic clay particles, which have week interfacial interaction with IIR. In the curing temperature range of 110–160°C, the former factor is likely more dominant, so that the strength of interaction between clay particles and IIR increased with curing temperature. When the curing temperature is over 160°C, deadsorption of organic surfactant becomes extremely severe not only resulting in the formation of more amount of inorganic clay but also decreasing the

TABLE II
Influence of Vulcanization Temperature (T_v) on Mechanical Performances of IIRCNs (IIR : OMC = 100 : 10)

T_v (°C)	M50[a] (MPa)	M100[a] (MPa)	M300[a] (MPa)	M500[a] (MPa)	Tensile strength (MPa)	Elongation at break (%)
110	0.51	0.64	1.03	1.65	7.6	795
120	0.53	0.73	1.25	2.16	16.3	788
130	0.56	0.75	1.29	2.32	18.6	777
140	0.57	0.78	1.40	2.71	20.4	770
150	0.51	0.73	1.40	2.74	17.2	721
160	0.47	0.69	1.47	3.14	13.5	673
170	0.55	0.78	1.54	3.14	13.9	688
180	0.56	0.74	1.49	2.78	18.6	745

[a] M50, M100, M300, and M400 represent modulus at 50, 100, 300, and 500% strain, respectively.

dispersion homogeneity. Furthermore, the further intercalation induced by curing reactions was also depressed due to excessive high-curing rate, decreasing the effective contact area between IIR and clay layers compared to IIRCN140 and IIRCN160. In consequence, the filler–rubber interaction decreased with curing temperature in the range of 160–180°C.

Figure 7 shows the changing trends of tensile strength and elongation at break of IIRCN with curing temperature. It can be seen that the changing trend of tensile strength could be divided into three regions: in region A (110–140°C), the tensile strength increases with curing temperature; in region B (140–160°C), it decreases with curing temperature; in region C (160–180°C), it increases again. The changing trend of elongation at break also could be divided into three regions: in region A, the elongation at break gradually decreases with curing temperature elevating; in region B, it still decrease, but the dropping rate is far greater; in region C, it increases with curing temperature considerably.

As well to known, the final tensile properties of rubber composites are influenced by many factors, for example, crosslinking density, filler dispersion state, and filler–rubber interaction. In region A, the crosslinking density and the filler–rubber interaction strength increase considerably with curing temperature [as shown in Figs. 1(b) and Fig. 6, respectively]. It not only depresses the mobility of rubber chains, causing reduction of elongation at break, but also enhances the efficiency of stress transfer, facilitating tensile-induced crystallization of IIR chains. The formed microcrystallites can retard cracks growing and delay fracture of the composite. Furthermore, Figure 2(b) displays that dispersion homogeneity of clay particles improved with curing temperature in region A, which also increases their ability for

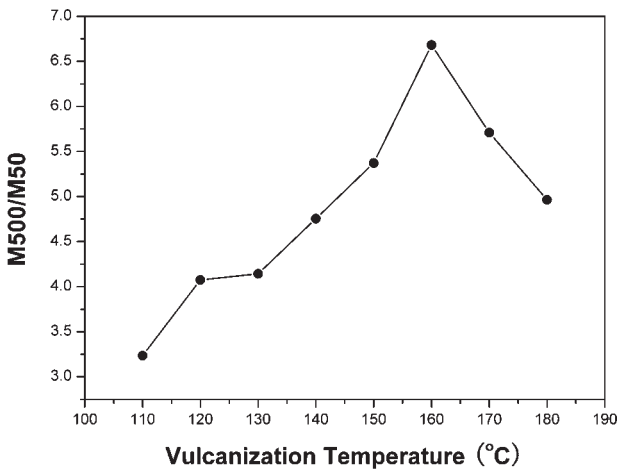

Figure 6 Influence of vulcanization temperature on reinforcement index (M500/M50) of IIRCN (IIR : OMC = 100 : 10).

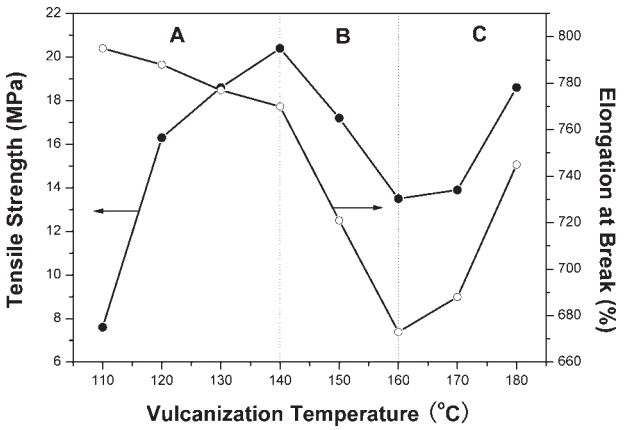

Figure 7 Changes of tensile strength and elongation at break of IIRCN (IIR : OMC = 100 : 10) with vulcanization temperature.

retarding crack growth. As a result, the tensile strength of IIRCN increases greatly with curing temperature, but elongation at break reduces slightly in region A. Figures 1(b) and 2(b) show that the crosslinking density and dispersion state of IIRCN did not change very much with curing temperature when it over 150°C, so that we mainly consider the filler–rubber interaction state for interpreting tensile-property changes with curing temperature in region of 140–180°C. In region B, the strength of interfacial interactions between clay particles and IIR still increases with curing temperature (Fig. 7). It has been reported that too strong rubber–filler bonding would confine the slippage of rubber chains on the filler surface and their orientation,[29] which would depress tensile-induced crystallization of IIR chains. Therefore, both the tensile strength and elongation at break of IIRCN decrease considerably with curing temperature in region B. In region C, the filler–rubber strength interaction decreases with curing temperature (Fig. 5) caused by severe deadsorption of surfactants of OMC [Fig. 2(b)]. For this reason, the ability of tensile-induced crystallization of IIR chains has been recovered to some extent with curing temperature increasing, and therefore both the tensile strength and elongation at break of IIRCN increase obviously in region C.

CONCLUSIONS

1. During sulfur vulcanization of IIRCNs, pressure, and curing reactions, reactions of amine intercalants with CAs play important roles on determining the final microstructures of cured IIRCNs. The reactions during initial curing period result in further intercalation of rubber chains into clay galleries and improve spatial dispersion of clay particles. High pressure leads

to the aggregation of clay layers to form larger clay agglomerates. Increasing curing rate by elevating temperature can reduce this aggregation. However, exorbitant curing temperatures (i.e., 160–180°C for this system) also strongly accelerate the reactions between amine intercalants with CAs, resulting in deadsorption of intercalants with the formation of larger amounts of inorganic clays and retarding further intercalation of IIR chains into silicate gallery induced by curing reactions.

2. Because the crosslinking density, filler dispersion state, and filler–rubber interactions are strongly influenced by curing temperature, the gas barrier and mechanical performances of IIRCN cured under different temperature are quite different.
3. Finally, authors propose some suggestions for preparing successful RCNs according to the results of this work. (a) If commercial OMC (the intercalants are usually organic amine) is used, the vulcanization system and parameters (i.e., curing temperature and pressure) must be carefully designed. Some studies[13,18–21] concerning this aspect have been performed. (b) The specific OMC for preparing RCNs should be developed, of which the intercalants do not react with CAs or interact with clay layers very strongly.

References

1. Karger-Kocsis, J.; Wu, C.-M. Polym Eng Sci 2004, 44, 1083.
2. Arroyo, M.; López-Manchado, M.A.; Valentín, J. L.; Carretero, J. Compos Sci Technol 2007, 67, 1330.
3. López-Manchado, M.A.; Valentín, J. L.; Carretero, J.; Barroso, F.; Arroyo, M. Euro Polym J 2007, 43, 4143.
4. Alexandre, M.; Dubios, P. Mater Sci Eng 2000, 28, 1.
5. Ray, S. S.; Okamoto, M. Prog Polym Sci 2003, 28, 1539.
6. Kim, J.-T.; Oh, T.-S.; Lee, D.-H. Polym Int 2003, 52, 1203.
7. Kim, J.-T.; Oh, T.-S.; Lee, D.-H. Polym Int 2003, 52, 1058.
8. Ma, J.; Xu, J.; Ren, J.-H.; Yu, Z.-Z.; Mai, Y.-W. Polymer 2003, 44, 4619.
9. Zhang, H.; Zhang, Y.; Peng, Z.; Zhang, Y. Polym Test 2004, 23, 217.
10. Gatos, K. G.; Sawanis, N. S.; Apostolov, A. A.; Thomann, R.; Karger-Kocsis, J. Macromol Mater Eng 2004, 289, 1079.
11. Schőn, F.; Thomanm, R.; Gronski, W. Macromol Symp 2002, 189, 105.
12. Gatos, K. G.; Thomann, R.; Karger-Kocsis, J. Polym Int 2004, 53, 1191.
13. Gatos, K. G.; Karger-Kocsis, J. Polymer 2005, 46, 3069.
14. Zhang, H.; Zhang, Y.; Peng, Z.-L.; Zhang, Y.-X. J Appl Polym Sci 2004, 92, 638.
15. Liang, Y.-R.; Lu, Y.-L.; Wu, Y.-P.; Ma, Y.; Zhang, L.-Q. Macromol Rapid Commun 2005, 26, 926.
16. Liang, Y.-R.; Ma, J.; Lu, Y.-L.; Wu, Y.-P.; Zhang, L.-Q.; Mai, Y.-W. J Polym Sci Part B: Polym Phys 2005, 43, 2653.
17. Lu, Y.-L.; Liang, Y.-R.; Wu, Y.-P.; Zhang, L.–Q. Macromol Mater Eng 2006, 291, 27.
18. Varghese, S.; Karger-Kocsis, J. J Appl Polym Sci 2004, 91, 813.
19. Usuki, A.; Kato, T. M. Polymer 2002, 43, 2185.
20. LeBaron, P. C.; Pinnavaia, T. J Chem Mater 2001, 13, 3760.
21. Gatos, K. G.; Százdi, L.; Pukánszky, B.; Karger-Kocsis, J. Macromol Rapid Commun 2005, 26, 915.
22. Hwang, W.-G.; Wei, K.-H.; Wu, C.–M. Polym Eng Sci 2004, 44, 2117.
23. Lu, Y.-L. Liang, Y.-R.; Wu, Y.-P.; Zhang, L.-Q. National Conference for Polymer Science of China Symposium 2005, Beijing, C-O-1630/p260.
24. Wu, Y.-P.; Jia, Q.-X.; Yu, D.-S.; Zhang, L.-Q. J Appl Polym Sci 2003, 89, 3855.
25. Sadhu, S.; Bhowmick, A. K. J Appl Polym Sci 2004, 92, 698.
26. Osman, M. A.; Mittal, V.; Morbidelli, M.; Suter, U. W. Macromolecules 2003, 36, 9851.
27. Osman, M. A.; Mittal, V.; Morbidelli, M.; Suter, U. W. Macromolecules 2004, 37, 7250.
28. Wang, Y.-Q.; Wu, Y.-P.; Zhang, H.-F.; Zhang, L.-Q.; Wang, B.; Wang, Z.-F. Macromol Rapid Commun 1973 2004, 25.
29. Sae-oui, P.; Sirisinha, C.; Thepsuwan, U.; Hatthapanit, K. Eur Polym J 2006, 42, 479.
30. Menon, A. R. R.; Pillai, C. K. S.; Nando, G. B. J Appl Polym Sci 1998, 68, 1303.
31. Edwards, D. C. J Mater Sci 1990, 25, 4175.